



Article

Assessment of the Long-Range NMR C,H Coupling of a Series of Carbazolequinone Derivatives

Matías Monroy-Cárdenas ^{1,2}, José A. Gavín ^{3,*} and Ramiro Araya-Maturana ^{1,2,*} 

¹ Interdisciplinary Group on Mitochondrial Targeting and Bioenergetics (MIBI), Talca 3480094, Chile; matias.monroy@utalca.cl

² Instituto de Química de Recursos Naturales, Universidad de Talca, Talca 3480094, Chile

³ Instituto Universitario de Bioorgánica “Antonio González” Departamento de Química Orgánica, Universidad de La Laguna, 38206 La Laguna, Tenerife, Spain

* Correspondence: jgavin@ull.edu.es (J.A.G.); raraya@utalca.cl (R.A.-M.)

Abstract: Synthesis, the complete ¹H- and ¹³C-NMR assignments, and the long-range C,H coupling constants (ⁿJ_{C,H}) of some hydrogen-deficient carbazolequinones, assessed by a J-HMBC experiment, are reported. In these molecules, the protons, used as entry points for assignments, are separated by several bonds with non-protonated atom carbons. Therefore, the use of long-range NMR experiments for the assignment of the spectra is mandatory; we used HSQC and HMBC. On the other hand, the measured heteronuclear (C,H) coupling constants (²J to ⁵J) allow us to choose the value of the long-range delay used in the HMBC experiment less arbitrarily in order to visualize a desired correlation in the spectrum. The chemical shifts and the coupling constant values can be used as input for assignments in related chemical structures.

Keywords: quinone; carbazolequinones; NMR spectroscopy; long-range C-H coupling; J-HMBC



Citation: Monroy-Cárdenas, M.; Gavín, J.A.; Araya-Maturana, R. Assessment of the Long-Range NMR C,H Coupling of a Series of Carbazolequinone Derivatives. *Int. J. Mol. Sci.* **2023**, *24*, 17450. <https://doi.org/10.3390/ijms242417450>

Academic Editors: Narimantas K. Cenias and Ilya A. Khodov

Received: 15 November 2023

Revised: 29 November 2023

Accepted: 1 December 2023

Published: 14 December 2023



Copyright: © 2023 by the authors. Licensee MDPI, Basel, Switzerland. This article is an open access article distributed under the terms and conditions of the Creative Commons Attribution (CC BY) license (<https://creativecommons.org/licenses/by/4.0/>).

1. Introduction

Molecular structure elucidation is at the basis of almost all of organic chemistry. The main tools needed to achieve this goal are nuclear magnetic resonance (NMR) spectroscopy and high-resolution mass spectrometry (HRMS). The two-dimensional (2D)-NMR experiments, based on the spin–spin coupling networks of the molecule, play a crucial role in structure elucidation [1]. Among them, heteronuclear long-range correlation experiments are essential. These experiments are the only way to connect molecular fragments through non-protonated carbons or heteroatoms. The oldest, but still the most widely used, is the HMBC experiment [2,3]. This pulse sequence consists of a few radiofrequency pulses, making it robust and the most sensitive [4]. The HMBC experiment allows structural information to be obtained using long-range correlation signals for C,H spin pairs. The detection of these correlation signals relies on the correct choice of NMR parameters, especially the long-range delay that can be adjusted while taking into account the magnitude of the coupling constants [5]. This delay is calculated as follows: $\Delta_2 = 1/(2 \text{ } ^nJ_{C,H})$. Since organic compounds have a range of ⁿJ_{C,H} values, usually from 2 to 15 Hz [6], Δ_2 should be at least equal to 100 ms. Generally, a delay shorter than the theoretical value is employed to avoid the decay of ¹H magnetization during this delay, particularly for large molecules. When the experiment is optimized for CH-long-range couplings ⁿJ_{C,H} in the range of 6–10 Hz, it provides access mainly to ³J_{C,H} correlations, whereas the often smaller ²J_{C,H} and ⁴J_{C,H} couplings generate weak or invisible correlation signals in the spectra [1,4,7]. However, the choice is generally made arbitrarily rather than from knowledge of the actual value of the couplings. Therefore, knowing the coupling constants in model molecules can help in choosing the adequate NMR parameters and, hence, correctly assigning the signals in the HMBC spectrum. This is because sometimes, four and even five-bond correlations, in addition to the common two and three-bond correlations observed using a standard value

of Δ_2 (60–80 ms), are observed. Correlations to four and even six bonds have been observed for diverse molecular structures and coupling pathways [1,6,8–15]. Some of them are as simple as ethyl crotonate, which, using a 65 ms delay [8], exhibits a five-bond correlation between the methyl protons of the alkoxy group and the C_α to the carbonyl group, a coupling pathway with a high degree of freedom. This is notable because the rigidity of the molecules has been argued as the reason we observed these non-common couplings. A special issue is the case of extremely hydrogen-deficient compounds, because their elucidation, in some cases, relies on these type of couplings. Complementary to HMBC, J-HMBC, among other NMR experiments, has been developed to visualize the very long-range connectivities [16–22]. The assignment of NMR spectra and measuring long-range C,H couplings provide insights into the adequate selection of parameters (mainly long-range delay in HMBC experiment) in the NMR of hydrogen-deficient molecules. These can also be used as input data for NMR calculations with theoretical methods, because they need to corroborate the accuracy of the data obtained by comparison with experimental results or combine the data to obtain information, for example, regarding conformational equilibrium in flexible molecules [23–25]. On the other hand, quinones have wide structural diversity [26] and are vastly distributed in nature, including in interstellar dust [27]. They have essential roles in the cell electron transport chain [28] and spark great interest in toxicology [29,30], medicinal chemistry [31–33], and agriculture as antifungals against phytopathogenic fungus [34–36]. Furthermore, quinones have relevance as dyes [37] and in energy storage, especially those with nitrogen atoms in their structures [38,39]. Among this last class of quinones, carbazole quinones have attracted interest owing to the bioactivities of some of its members [40,41]. Murrayaquinone A, among others, has shown promising cytotoxicity [41]. Calothrixin B (Figure 1) has shown a high level of in vitro cytotoxicity against the HeLa cancer cell line by interacting with human topoisomerase I and generating reactive oxygen species [42]. Some carbazolequinones show inhibitory effects on lipopolysaccharide and interferon-gamma-induced nitric oxide production in cells [43].

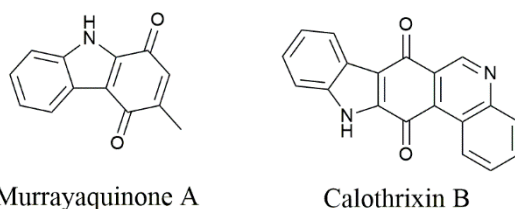


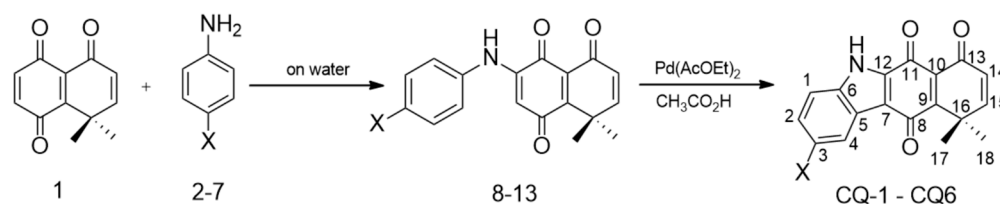
Figure 1. Chemical structures of Murrayaquinone A and Calothrixin B.

Our interest in biologically active quinones has led us to achieve their unequivocal structural characterization using NMR [44], assess the antitumor activity of isoquinolinequinones [45], and study carbazolequinones via mass spectrometry [46]. This work aims to study some hydrogen-deficient *o*-carbonyl carbazolequinone derivatives, whose molecular skeleton has been previously studied by us [46], in addition to measuring their long-range heteronuclear coupling constants and evaluating the effects of the substituents on them.

2. Results

2.1. Synthesis

The compounds were obtained following the synthetic sequence depicted in Scheme 1, in which the first step is the on-water C-N oxidative coupling of quinone 1 with aromatic amines previously described by us [47]. In the second step, amino quinones were used as starting products in an oxidative coupling with palladium acetate under a nitrogen atmosphere, generating the corresponding *o*-carbonyl carbazolequinones CQ-1–CQ-6, following a procedure which has previously been described [46].



Scheme 1. Synthesis of the studied carbazolequinones and numbering used in their structures. Compounds CQ-1 and CQ-4 have been previously described [46].

2.2. Complete NMR Assignments of the ^{13}C NMR

Tables 1 and 2 show the assignments of these spectra, which were not straightforward because the central regions of these structures consist only of carbonyl and quaternary carbon atoms aside from nitrogen atoms. The resonances of these atoms must be correlated via long-range $J(\text{CH})$ by the concerted use of ^1H -detected one bond (C-H) heteronuclear single quantum coherence (HSQC) [48] and long-range C-H heteronuclear multiple bond connectivity (HMBC) [2].

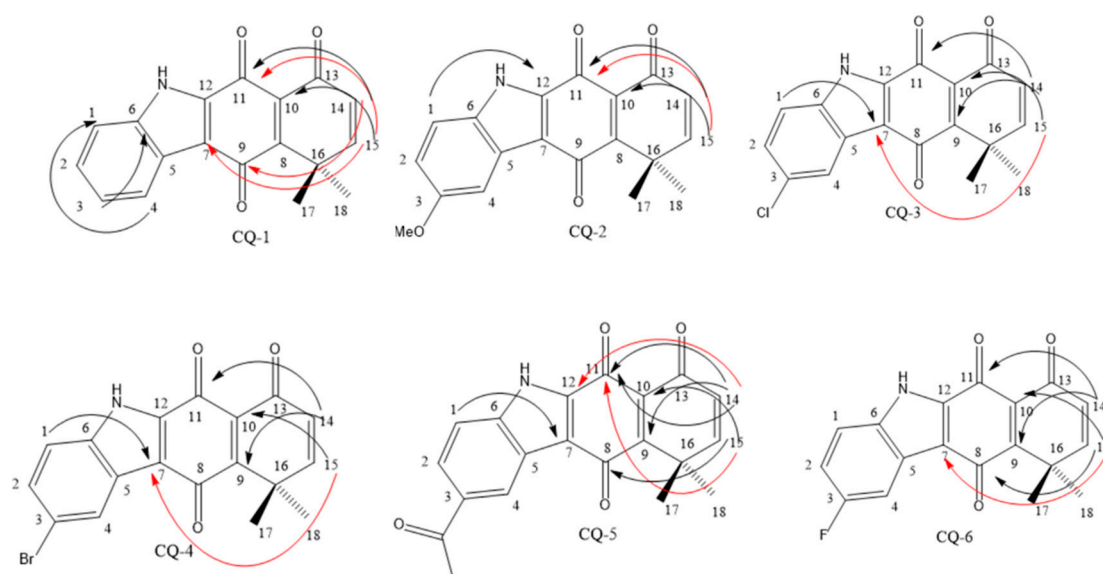
Table 1. ^{13}C assignments of the studied compounds.

Compound	CQ-1	CQ-2	CQ-3	CQ-4	CQ-5	CQ-6
X	H	OMe	Cl	Br	COMe	F
C1	114.4	115.6	116.2	116.5	114.4	116.1
C2	127.1	118.4	127.2	129.8	126.5	115.9
C3	124.6	157.6	129.1	117.1	133.3	160.1
C4	122.4	102.3	121.3	124.4	123.9	106.8
C5	123.9	123.9	124.8	125.4	123.4	124.4
C6	138.2	138.2	136.6	136.8	140.4	134.9
C7	116.6	116.6	116.0	115.8	117.5	116.4
C8	183.1	183.1	183.0	183.0	183.2	182.9
C9	159.0	159.0	158.9	158.9	158.8	159.0
C10	130.3	130.4	130.4	130.4	130.3	130.4
C11	178.1	177.8	177.9	177.9	177.9	177.9
C12	135.7	135.6	136.7	136.5	137.2	137.0
C13	183.6	183.7	183.5	183.5	183.5	183.6
C14	127.0	127.0	127.0	127.0	127.0	127.0
C15	158.6	158.6	158.6	158.6	158.7	158.6
C16	39.5	39.5	39.5	39.5	39.5	39.5
gem-Me	26.7	26.6	26.6	26.6	26.6	26.6
OMe		55.8				
MeCO					31.1	

The ^1H NMR spectra of the tricyclic skeleton of the six carbazolequinones show the protons of the AB system corresponding to the enone moiety 14-H and 15-H, where 15-H resonates at a lower field due to the resonance effect of the carbonyl group. On the other hand, the aromatic protons 4-H and 1-H are easily distinguishable from each other because of the deshielding effect that the carbonyl group at C8 exerts over 4-H. In addition, for CQ-2 to CQ-6, the multiplicity of the aromatic resonance also allows for assignment. Based on this, and using the HSQC experiment, the protonated carbons were identified. Then, via the HMBC method, the non-protonated carbons were assigned. Figure 2 shows some of the long-range correlations ($^4J_{\text{C,H}}$ and $^5J_{\text{C,H}}$) that allowed both fragments to be joined.

Table 2. ^1H assignments of the studied compounds.

	CQ-1	CQ-2	CQ-3	CQ-4	CQ-5	CQ-6
H1	7.56	7.46	7.58	7.53	7.64	7.59
H2	7.42	7.06	7.44	7.56	8.00	7.31
H3	7.35	-	-	-	-	-
H4	8.11	7.52	8.06	8.22	8.70	7.77
H14	6.26	6.25	6.26	6.27	6.28	6.26
H15	7.01	7.06	7.02	7.02	7.02	7.01

**Figure 2.** Key long-range correlations ($^4J_{\text{C,H}}$ and $^5J_{\text{C,H}}$) observed. The red arrows show the $^5J_{\text{C,H}}$ coupling, and the black arrows correspond to $^4J_{\text{C,H}}$ coupling.

Tables 3–8 show the measured coupling constants (absolute values in Hz) for the studied carbazolequinones, obtained from J-HMBC experiments [16].

Table 3. Coupling constants for CQ-1.

H ₄	$^2J_{\text{C}_3}$ 2.1	$^3J_{\text{C}_7}$ 2.0	$^3J_{\text{C}_2}$ 5.6	$^3J_{\text{C}_6}$ 7.3	
H ₁	$^3J_{\text{C}_3}$ 9.1	$^4J_{\text{C}_{12}}$ 6.1	$^4J_{\text{C}_4}$ 2.0		
H ₂	$^2J_{\text{C}_3}$ 1.9	$^3J_{\text{C}_4}$ 4.9	$^3J_{\text{C}_6}$ 10.0		
H ₁₅	$^2J_{\text{C}_{16}}$ 2.5	$^3J_{\text{C}_{17/18}}$ 2.4	$^3J_{\text{C}_9}$ 7.2	$^3J_{\text{C}_{13}}$ 10.1	$^4J_{\text{C}_{10}}$ 2.0
H ₁₄	$^3J_{\text{C}_{16}}$ 7.5	$^3J_{\text{C}_{10}}$ 4.1	$^4J_{\text{C}_{17/18}}$ 2.0	$^4J_{\text{C}_{11}}$ 2.1	$^4J_{\text{C}_{11}}$ 2.1
H _{17/18}	$^3J_{\text{C}_{17/18}}$ 4.9	$^2J_{\text{C}_{16}}$ 3.8	$^4J_{\text{C}_{14}}$ 2.3	$^3J_{\text{C}_9}$ 3.6	

Table 4. Coupling constants for CQ-2.

H ₄	$^2J_{\text{C}_3}$ 2.9	$^3J_{\text{C}_6}$ 7.4	$^4J_{\text{C}_1}$ 2.0				
H ₁	$^3J_{\text{C}_5}$ 2.9	$^3J_{\text{C}_3}$ 11.0	$^4J_{\text{C}_4}$ 2.6	$^4J_{\text{C}_7}$ 5.7			
H ₂	$^2J_{\text{C}_1}$ 2.0	$^2J_{\text{C}_3}$ 2.3	$^3J_{\text{C}_4}$ 5.6	$^3J_{\text{C}_6}$ 10.0			
H ₁₅	$^2J_{\text{C}_{16}}$ 2.3	$^3J_{\text{C}_{17/18}}$ 2.1	$^3J_{\text{C}_9}$ 7.3	$^3J_{\text{C}_8}$ 2.8	$^3J_{\text{C}_{13}}$ 10.1	$^4J_{\text{C}_{10}}$ 2.0	$^5J_{\text{C}_7}$ 2.3
H ₁₄	$^2J_{\text{C}_{13}}$ 2.1	$^3J_{\text{C}_{16}}$ 7.5	$^3J_{\text{C}_{10}}$ 4.2	$^4J_{\text{C}_{17/18}}$ 2.1	$^4J_{\text{C}_9}$ 2.2	$^4J_{\text{C}_{11}}$ 2.5	
H _{17/18}	$^2J_{\text{C}_{16}}$ 3.3	$^3J_{\text{C}_{17/18}}$ 4.9	$^3J_{\text{C}_{15}}$ 3.7				

Table 5. Coupling constants for CQ-3.

HN	${}^2J_{C_{12}}$ 5.6	${}^2J_{C_6}$ 3.1	${}^3J_{C_5}$ 2.9	${}^3J_{C_7}$ 4.9			
H ₄	${}^3J_{C_7}$ 2.6	${}^3J_{C_2}$ 7.5	${}^3J_{C_6}$ 6.8	${}^4J_{C_1}$ 2.8			
H ₁	${}^2J_{C_2}$ 3.6	${}^3J_{C_5}$ 5.6					
H ₂	${}^2J_{C_1}$ 3.4	${}^3J_{C_4}$ 8.0	${}^3J_{C_6}$ 9.7				
H ₃	${}^2J_{C_2}$ 2.5	${}^3J_{C_1}$ 8.2	${}^3J_{C_5}$ 9.1	${}^4J_{C_6}$ 2.5			
H ₁₅	${}^2J_{C_{16}}$ 2.8	${}^3J_{C_{17/18}}$ 2.1	${}^3J_{C_9}$ 7.1	${}^3J_{C_{13}}$ 10.5	${}^4J_{C_{10}}$ 1.8	${}^4J_{C_8}$ 2.4	${}^5J_{C_7}$ 2.3
H ₁₄	${}^2J_{C_{13}}$ 1.8	${}^3J_{C_{16}}$ 7.4	${}^3J_{C_{10}}$ 4.1	${}^4J_{C_{17/18}}$ 1.8	${}^5J_{C_9}$ 2.0	${}^4J_{C_{11}}$ 1.8	
H _{17/18}	${}^2J_{C_{16}}$ 3.4	${}^3J_{C_{17/18}}$ 4.3	${}^3J_{C_9}$ 3.5	${}^4J_{C_{14}}$ 1.8			

Table 6. Coupling constants for CQ-4.

H ₄	${}^2J_{C_3}$ 3.5	${}^3J_{C_7}$ 2.1	${}^3J_{C_2}$ 4.6	${}^3J_{C_6}$ 8.0			
H ₁	${}^3J_{C_5}$ 5.3	${}^3J_{C_3}$ 10.0	${}^4J_{C_{12}}$ 5.8				
H ₂	${}^2J_{C_3}$ 2.2	${}^3J_{C_4}$ 4.5	${}^3J_{C_6}$ 9.0				
H ₁₅	${}^2J_{C_{16}}$ 3.0	${}^3J_{C_{17/18}}$ 3.2	${}^3J_{C_9}$ 7.5	${}^3J_{C_{13}}$ 10.0	${}^4J_{C_{10}}$ 2.7	${}^5J_{C_7}$ 2.1	
H ₁₄	${}^2J_{C_{13}}$ 3.0	${}^3J_{C_{16}}$ 8.0	${}^3J_{C_{10}}$ 3.5	${}^4J_{C_{17/18}}$ 2.9	${}^4J_{C_9}$ 3.0	${}^4J_{C_{11}}$ 3.4	
H _{17/18}	${}^2J_{C_{16}}$ 3.1	${}^3J_{C_{17/18}}$ 3.5	${}^3J_{C_9}$ 3.5				

Table 7. Coupling constants for CQ-5.

H ₄	${}^3J_{C_7}$ 2.2	${}^3J_{C_2}$ 7.3	${}^3J_{C_6}$ 7.6	${}^3J_{CO}$ 3.6	${}^4J_{C_1}$ 2.8		
H ₁	${}^3J_{C_3}$ 7.0	${}^3J_{C_5}$ 5.3	${}^4J_{CO}$ 1.9	${}^5J_{C_8}$ 2.0			
H ₂	${}^3J_{C_4}$ 6.0	${}^3J_{C_6}$ 10.1	${}^3J_{CO}$ 2.8				
H ₁₅	${}^2J_{C_{16}}$ 2.7	${}^3J_{C_{17/18}}$ 2.1	${}^3J_{C_9}$ 7.2	${}^3J_{C_{13}}$ 10.4	${}^4J_{C_{10}}$ 2.0	${}^4J_{C_8}$ 3.0	
H ₁₄	${}^2J_{C_{13}}$ 1.9	${}^3J_{C_{16}}$ 7.6	${}^3J_{C_{10}}$ 3.9	${}^4J_{C_{17/18}}$ 3.0	${}^4J_{C_9}$ 2.0	${}^4J_{C_{11}}$ 2.1	${}^5J_{C_{12}}$ 3.0
H _{17/18}	${}^2J_{C_{16}}$ 3.7	${}^3J_{C_{17/18}}$ 5.0	${}^3J_{C_9}$ 4.0				
CH ₃ -CO	${}^2J_{CO}$ 6.0						

Table 8. Coupling constants for CQ-6.

H ₄	${}^2J_{C_3}$ 5.0	${}^2J_{C_5}$ 5.0	${}^3J_{C_7}$ 2.0	${}^3J_{C_6}$ 7.6			
H ₁	${}^3J_{C_3}$ 4.4	${}^3J_{C_5}$ 6.1	${}^4J_{C_4}$ 2.3				
H ₂	${}^2J_{C_3}$ 4.1	${}^3J_{C_6}$ 10.1	${}^3J_{C_4}$ 3.9	${}^4J_{C_5}$ 4.1			
H ₁₅	${}^2J_{C_{16}}$ 2.2	${}^3J_{C_{17/18}}$ 2.0	${}^3J_{C_9}$ 7.1	${}^3J_{C_{13}}$ 10.5	${}^4J_{C_{10}}$ 2.0	${}^4J_{C_8}$ 2.7	${}^5J_{C_7}$ 2.3
H ₁₄	${}^2J_{C_{13}}$ 2.1	${}^3J_{C_{16}}$ 7.7	${}^3J_{C_{10}}$ 4.1	${}^4J_{C_{17/18}}$ 2.0	${}^4J_{C_9}$ 2.0	${}^4J_{C_{11}}$ 2.5	
H _{17/18}	${}^2J_{C_{16}}$ 3.6	${}^3J_{C_{17/18}}$ 4.8	${}^3J_{C_9}$ 3.9				

3. Discussion

The NMR spectra of the tricyclic skeleton of the six carbazolequinones were assigned as previously discussed. All molecules, except CQ-2, exhibited five-bond C,H coupling between H15 and C7 of 2–3 Hz, in the same range of several four-bond correlations. However, CQ-3 and CQ-6 also exhibited ${}^4J_{C,H}$ of 5.7 and 4.1 Hz. The 3J had values in the broad range of 2.0 to 11 Hz, and the two bond correlations ranged between 1.8 and 5.6 Hz. This wide dispersion of the coupling constant values makes it difficult to predict a small range for the value of a constant. Therefore, the data obtained from reference compounds

like these can be used as input data for assigning similar structures through experimental procedures or theoretical calculations.

4. Materials and Methods

NMR spectra were recorded on a Bruker Avance III 600 NMR spectrometer equipped with a 5 mm TCI cryogenic probe using 5 mm NMR tubes in dimethyl sulfoxide solutions. Chemical shifts were reported as ppm downfield from TMS for ^1H NMR, and as relative to the central DMSO- d_6 resonance (39.4 ppm) for ^{13}C NMR. Melting points were uncorrected and were measured using an Electrothermal 9100 apparatus. High resolution mass spectra (HRMS) were obtained using a high-resolution magnetic trisector (EBE) mass analyzer. Commercially available starting materials and solvents were used without further purification. Silica gel 60 (70–230 mesh) and alu-Foil 60 F254 were used for column chromatography and analytical TLC, respectively.

Synthesis of Carbazolequinones: General Procedure

In a Schlenk tube, under an inert atmosphere, a mixture of one equivalent of the respective anilinoquinone and one equivalent of $\text{Pd}(\text{OAc})_2$ in glacial acetic acid was heated under reflux for 4 h, and then filtered. The filtered mixture was extracted 3 times with ethyl acetate and washed with a sodium bicarbonate solution; the organic phase was dried with anhydrous sodium sulfate and then evaporated under vacuum. Column chromatography on silica gel with hexane: ethyl acetate 1:1 as the eluent allowed us to obtain pure carbazolequinones.

10,10-dimethyl-5*H*-benzo[*b*]carbazole-6,7,11(10*H*)-trione (CQ-1) [46]

A total of 60 mg (0.24 mmol) of 3-anilino-8,8-dimethylnaphthalene-1,4,5(8*H*)-trione and $\text{Pd}(\text{OAc})_2$ 45 mg (0.18 mmol) in glacial acetic acid (4 mL) yielded 32 mg of CQ-1 (54% yield). ^1H NMR (600.23 MHz, DMSO- d_6) δ : 1.62 (s, 6H, 2XCH $_3$), 6.26 (d, J = 10 Hz, 1H, 14-H), 7.01 (d, J = 10 Hz, 1H, 15-H), 7.35 (dd, J_1 = 8.2 Hz, J_2 = 7.9 Hz, 1H, 3-H), 7.42 (dd, J_1 = 8.2 Hz, J_2 = 7.9 Hz, 1H, 2-H), 7.56 (d, J = 8.2 Hz, 1H, 1 o 4-H), 8.11 (d, J = 7.9 Hz, 1H, 1 o 4-H), 12.90 (s, 1H). ^{13}C NMR (150.93 MHz, DMSO- d_6) δ : 26.68 (2XCH $_3$), 114.39, 116.82, 122.41, 123.91, 124.57, 127.04, 127.12, 130.27, 135.68, 138.17, 158.60, 158.99, 178.12, 183.14, 183.65. IR(KBr): 3237, 1683, 741 cm^{-1} . M.p.: 297–299 °C. HRMS (ESI) m/z : calculated for $\text{C}_{18}\text{H}_{13}\text{NO}_3$ M^+ 291.0895, 291.0894 was found.

2-methoxy-10,10-dimethyl-5*H*-benzo[*b*]carbazole-6,7,11(10*H*)-trione (CQ-2)

A total of 58 mg of 3-(4-methoxyphenylamino)-8,8-dimethylaminonaphthalene-1,4,5-(8*H*)-trione (0.18 mmol) reacted with 40 mg of palladium acetate (II) (0.24 mmol), yielding 32 mg of CQ-2 (55% Yield). ^1H NMR (600.23 MHz, DMSO- d_6) δ : 1.62 (s, 6H, 2XCH $_3$), 3.85 (s, 3H, O-CH $_3$), 6.25 (d, J = 10 Hz, 1H, 14-H), 7.00 (d, J = 10 Hz, 1H, 15-H), 7.06 (dd, J_1 = 8.8 Hz, J_2 = 2 Hz, 1H, 3-H), 7.46 (d, J = 9 Hz, 1H, 4-H), 7.52 (d, J = 2 Hz, 1H, 1-H), 12.83 (s, 1H). ^{13}C NMR (150.93 MHz, DMSO- d_6) δ : 26.66 (2XCH $_3$), 55.86 (O-CH $_3$), 102.29, 115.60, 116.40, 118.39, 124.95, 127.03, 130.42, 133.39, 135.64, 157.61, 158.60, 159.13, 177.79, 182.91, 183.73. IR(KBr): 3253, 1687, 836 cm^{-1} . M.p.: 278–280 °C. HRMS (ESI) m/z : calculated for $\text{C}_{19}\text{H}_{15}\text{NO}_4$ M^+ 321.1001, 321.1007 was found.

2-chloro-10,10-dimethyl-5*H*-benzo[*b*]carbazole-6,7,11(10*H*)-trione (CQ-3)

A total of 180 mg of 3-((4-chlorophenyl)amino)-8,8-dimethylnaphthalen-1,4,5(8*H*)-trione (0,548 mmol) and 123 mg of palladium acetate (II) (0,548 mmol) allowed us to obtain 77 mg of CQ-3 (43% yield). ^1H -NMR (600.23 MHz, DMSO- D_6) δ 1.61 (s, 6H, 2XCH $_3$), 6.26 (d, J = 10 Hz, 1H, 8-H), 7.02 (d, J = 10 Hz, 1H, 9-H), 7.44 (dd, J_1 = 9 Hz, J_2 = 2 Hz, 1H, 3-H), 7.58 (d, J = 9 Hz, 1H, 4-H), 8.06 (d, J = 2 Hz, 1H, 1-H), 13.10 (s, 1H, NH). ^{13}C -NMR (150.93 MHz, DMSO- d_6) δ 26.62 (2XCH $_3$), 115.96, 116.19, 121.27, 124.79, 127.04, 127.25, 129.08, 130.38, 136.61, 136.69, 158.61, 158.91, 177.93, 182.96, 183.56. M.p.: 248–250 °C. HRMS (ESI) m/z : calculated for $\text{C}_{18}\text{H}_{12}\text{ClNO}_3$ M^+ 325.0506, 325.0495 was found.

2-bromo-10,10-dimethyl-5*H*-benzo[*b*]carbazole-6,7,11(10*H*)-trione (CQ-4) [46]

A total of 41 mg of 3-[(4-bromophenyl)amino]-8,8-dimethylnaphthalene-1,4,5(8*H*)-trione (0,11 mmol) and $\text{Pd}(\text{OAc})_2$ (25 mg, 0,11 mmol) yielded 17 mg of CQ-4 (39%). ^1H NMR (600.23 MHz, DMSO- d_6) δ : 1.61 (s, 6H, 2XCH $_3$), 6.27 (d, J = 9.9 Hz, 1H, 14-H), 7.02 (d,

$J = 9.9$ Hz, 1H, 15-H), 7.53 (d, $J = 8.6$ Hz, 1H, 4-H), 7.56 (dd, $J_1 = 8.8$ Hz, $J_2 = 1.8$ Hz, 1H, 3-H), 8.22 (d, $J = 1.3$ Hz, 1H, 1-H), 13.10 (s, 1H, NH). ^{13}C NMR (150.93 MHz, DMSO- d_6) δ 187.55, 181.64, 181.44, 178.41, 177.03, 159.62, 145.04, 144.27, 137.91, 130.74, 130.25, 128.01, 126.40, 118.03, 112.43, 31.24, 27.63. IR: 3220, 1690, 817 cm^{-1} . M.p.: 272–274 °C. HRMS (ESI) m/z : calculated for $\text{C}_{18}\text{H}_{12}\text{BrNO}_3 \text{M}^+$ 369.0001, 368.9987 was found.

2-acetyl-10,10-dimethyl-5H-benzo[b]carbazole-6,7,11(10H)-trione (CQ-5)

3-((4-acetylphenyl)amino)-8,8-dimethylnaphthalen-1,4,5(8H)-trione (139 mg, 0.415 mmol) and palladium acetate (II) (93 mg, 0.415 mmol) reacted, yielding 47 mg of CQ-5 (34% yield). ^1H -NMR (600.23 MHz, DMSO- d_6) δ 1.63 (s, 6H, 2XCH₃), 2.67 (s, 3H, CH₃CO), 6.28 (d, $J = 10$ Hz, 8-H), 7.02 (d, $J = 10$ Hz, 9-H), 7.64 (d, $J = 9$ Hz, 1H, 4-H), 8.00 (dd, $J_1 = 2$ Hz, $J_2 = 9$ Hz, 1H, 3-H), 8.70 (d, $J = 2$ Hz, 1H, 1-H), 13.19 (s, 1H, NH). ^{13}C -NMR (150.93 MHz, DMSO- d_6) δ 26.63, 27.25, 114.43, 117.45, 123.43, 123.95, 126.54, 127.05, 130.26, 133.28, 137.25, 140.45, 158.66, 158.81, 177.95, 183.23, 183.56. M.p.: 252–254 °C. HRMS (ESI) m/z : calculated for $\text{C}_{20}\text{H}_{15}\text{NO}_4 \text{M}^+$ 333.1001, 333.0995 was found.

2-fluoro-10,10-dimethyl-5H-benzo[b]carbazole-6,7,11(10H)-trione (CQ-6)

3-((4-fluorophenyl)amino)-8,8-dimethylnaphthalen-1,4,5(8H)-trione (220 mg, 0.7 mmol) reacted with palladium acetate (II) (151 mg, 0.7 mmol), of CQ-6 17 (97 mg, 45%). ^1H -NMR (600.23 MHz, DMSO) δ 1.61 (s, 6H, 2XCH₃), 6.26 (d, $J = 10$ Hz, 1H, 8-H), 7.01 (d, $J = 10$ Hz, 1H, 9-H), 7.31 (ddd, $J_1 = 9$ Hz, $J_2 = 9$ Hz, $J_3 = 3$ Hz, 1H, 3-H), 7.59 (dd, $J_1 = 9$ Hz, $J_2 = 4$ Hz, 1H, 4-H), 7.77 (dd, $J_1 = 9$ Hz, $J_2 = 3$ Hz, 1H, 1-H), 13.05 (s, 1H, NH). ^{13}C -NMR (150.93 MHz, DMSO) δ 26.63, 106.78, 106.95, 115.84, 116.01, 116.13, 116.19, 116.60, 116.64, 124.29, 124.36, 127.03, 130.42, 134.89, 137.00, 158.62, 159.00, 159.30, 160.88, 177.89, 182.89, 183.60. M.p.: 251–253 °C. HRMS (ESI) m/z : calculated for $\text{C}_{18}\text{H}_{12}\text{FNO}_3 \text{M}^+$ 309.0801, 309.0790 was found.

Author Contributions: R.A.-M. designed the research; M.M.-C. performed the synthesis of the compounds, J.A.G. performed the NMR experiments. R.A.-M. and J.A.G. analyzed the data. R.A.-M. wrote the paper. All authors have read and agreed to the published version of the manuscript.

Funding: This research was funded by ANID/FONDECYT grant N° 1221874, and was also supported by ANID-Anillo ACT210097. We also thank the Nuclear Magnetic Resonance Service of Universidad de La Laguna for allocating instrument time to this project.

Institutional Review Board Statement: Not applicable.

Informed Consent Statement: Not applicable.

Data Availability Statement: Data contained within the article.

Conflicts of Interest: The authors declare no conflict of interest.

References

1. Saurí, J.; Liu, Y.; Parella, T.; Williamson, R.T.; Martin, G.E. Selecting the Most Appropriate NMR Experiment to Access Weak and/or Very Long-Range Heteronuclear Correlations. *J. Nat. Prod.* **2016**, *79*, 1400–1406. [[CrossRef](#)] [[PubMed](#)]
2. Bax, A.; Summers, M.F. ^1H and ^{13}C Assignments from Sensitivity-Enhanced Detection of Heteronuclear Multiple-Bond Connectivity by 2D Multiple Quantum NMR. *J. Am. Chem. Soc.* **1986**, *108*, 2093–2094. [[CrossRef](#)]
3. Bax, A.; Marion, D. Improved Resolution and Sensitivity in ^1H -Detected Heteronuclear Multiple-Bond Correlation Spectroscopy. *J. Magn. Reson.* **1988**, *78*, 186–191. [[CrossRef](#)]
4. Furrer, J. A Comprehensive Discussion of HMBC Pulse Sequences, Part 1: The Classical HMBC. *Concepts Magn. Reson. Part A* **2012**, *40A*, 101–127. [[CrossRef](#)]
5. Reynolds, W.F.; Enriquez, R.G. Choosing the Best Pulse Sequences, Acquisition Parameters, Postacquisition. *J. Nat. Prod.* **2002**, *65*, 221–244. [[CrossRef](#)]
6. Araya-Maturana, R.; Pessoa-Mahana, H.; Weiss-López, B. Very Long-Range Correlations ($\text{NJC}, \text{H } n > 3$) in HMBC Spectra. *Nat. Prod. Commun.* **2008**, *3*, 445–450. [[CrossRef](#)]
7. Williamson, R.T.; Buevich, A.V.; Martin, G.E.; Parella, T. LR-HSQMBC: A Sensitive NMR Technique to Probe Very Long-Range Heteronuclear Coupling Pathways. *J. Org. Chem.* **2014**, *79*, 3887–3894. [[CrossRef](#)]
8. Araya-maturana, R.; Gavín-sazatornil, J.A.; Heredia-moya, J.; Pessoa-Mahana, H.; Weiss-lópez, B. Long-Range Correlations ($n_j \text{C}, \text{H } n > 3$) in the HMBC Spectra of 3-(4-Oxo-4H-chromen-3-yl)-acrylic Acid Ethyl Esters. *J. Braz. Chem. Soc.* **2005**, *16*, 657–661. [[CrossRef](#)]

9. Buevich, A.V.; Williamson, R.T.; Martin, G.E. NMR Structure Elucidation of Small Organic Molecules and Natural Products: Choosing ADEQUATE vs HMBC. *J. Nat. Prod.* **2014**, *77*, 1942–1947. [[CrossRef](#)]
10. Becerra-Martínez, E.; Pérez-Hernández, N.; Sánchez-Zavala, M.; Meléndez-Rodríguez, M.; Aristeo-Domínguez, A.; Suárez-Castillo, O.R.; Joseph-Nathan, P. Equilibrating Magnetic Dispersion and Magnet Homogeneity for the High-Resolution Proton Nuclear Magnetic Resonance of Monosubstituted Naphthalenes. *Spectrosc. Lett.* **2022**, *55*, 424–436. [[CrossRef](#)]
11. Hollenberg, M.D. Proteinase-Activated Receptors (PARs): An Evolving Hormonal System. *Drug Dev. Res.* **2003**, *59*, 334–335. [[CrossRef](#)]
12. Wang, X.-Y.; Yang, H.-H.; Chang, L.-K.; Chiu, T.-H.; Liu, F.-C.; Lin, I.J.B. Synthesis and Structures of Benzyl- and Amido-Substituted N-Heterocyclic Palladium Carbene. *Chem. Sel.* **2022**, *7*, e202201700. [[CrossRef](#)]
13. Vien, L.T.; Hanh, T.T.H.; Quang, T.H.; Cuong, N.T.; Cuong, N.X.; Oh, H.; Van Sinh, N.; Nam, N.H.; Minh, C. Van Oroxindols A and B, Two Novel Secoabietane Diterpenoids from *Oroxylum Indicum*. *Phytochem. Lett.* **2020**, *40*, 101–104. [[CrossRef](#)]
14. Burns, D.C.; Reynolds, W.F. Minimizing the Risk of Deducing Wrong Natural Product Structures from NMR Data. *Magn. Reson. Chem.* **2021**, *59*, 500–533. [[CrossRef](#)] [[PubMed](#)]
15. Surup, F.; Wiebach, V.; Kuhnert, E.; Stadler, M. Truncaquinones A and B, Asterriquinones from *Annulohyphoxylon Truncatum*. *Tetrahedron Lett.* **2016**, *57*, 2183–2185. [[CrossRef](#)]
16. Schulte-Herbrüggen, T.; Meissner, A.; Papanikos, A.; Meldal, M.; Sørensen, O.W. Optimizing delays in the MBOB, broadband HMBC, and broadband XLOC NMR pulse sequences. *J. Magn. Reson.* **2002**, *156*, 282–294. [[CrossRef](#)] [[PubMed](#)]
17. Furihata, K.; Seto, H. Decoupled HMBC (D-HMBC), an Improved Technique of HMBC. *Tetrahedron Lett.* **1995**, *36*, 2817–2820. [[CrossRef](#)]
18. Furihata, K.; Seto, H. 3D-HMBC, a New NMR Technique Useful for Structural Studies of Complicated Molecules. *Tetrahedron Lett.* **1996**, *37*, 8901–8902. [[CrossRef](#)]
19. Furihata, K.; Seto, H. Constant Time HMBC (CT-HMBC), a New HMBC Technique Useful for Improving Separation of Cross Peaks. *Tetrahedron Lett.* **1998**, *39*, 7337–7340. [[CrossRef](#)]
20. Hadden, C.E.; Martin, G.E.; Krishnamurthy, V.V. Improved Performance Accordion Heteronuclear Multiple-Bond Correlation Spectroscopy—IMPEACH-MBC. *J. Magn. Reson.* **1999**, *140*, 274–280. [[CrossRef](#)]
21. Hadden, C.E.; Martin, G.E.; Krishnamurthy, V.V. Constant Time Inverse-Detection Gradient Accordion Rescaled Heteronuclear Multiple Bond Correlation Spectroscopy: CIGAR-HMBC. *Magn. Reson. Chem.* **2000**, *38*, 143–147. [[CrossRef](#)]
22. Wagner, R.; Berger, S. ACCORD-HMBC: A Superior Technique for Structural Elucidation. *Magn. Reson. Chem.* **1998**, *36*, S44–S46. [[CrossRef](#)]
23. Marcarino, M.O.; Zanardi, M.M.; Cicetti, S.; Sarotti, A.M. NMR calculations with quantum methods: Development of new tools for structural elucidation and beyond. *Acc. Chem. Res.* **2020**, *53*, 1922–1932. [[CrossRef](#)] [[PubMed](#)]
24. Plazinski, W.; Angles d’Ortoli, T.; Widmalm, G. Conformational flexibility of the disaccharide β -l-Fucp-(1 \rightarrow 4)- α -d-Glcp-OMe as deduced from NMR spectroscopy experiments and computer simulations. *Org. Biomol. Chem.* **2023**, *21*, 6979–6994. [[CrossRef](#)] [[PubMed](#)]
25. Adamson, J.; Nazarski, R.B.; Jarvet, J.; Pehk, T.; Aav, R. Shortfall of B3LYP in Reproducing NMR JCH Couplings in Some Isomeric Epoxy Structures with Strong Stereoelectronic Effects: A Benchmark Study on DFT Functionals. *ChemPhysChem* **2018**, *19*, 631–642. [[CrossRef](#)]
26. Thomson, R.H. *Naturally Occurring Quinones IV*; Blackie Academic: London, UK, 1997.
27. Krueger, F.R.; Werther, W.; Kissel, J.; Schmid, E.R. Assignment of quinone derivatives as the main compound class composing ‘interstellar’ grains based on both polarity ions detected by the ‘Cometary and Interstellar Dust Analyser’ (CIDA) onboard the spacecraft STARDUST. *Rapid Commun. Mass Spectrom.* **2004**, *18*, 103–111. [[CrossRef](#)] [[PubMed](#)]
28. Monroy-Cárdenas, M.; Andrades, V.; Almarza, C.; Vera, M.J.; Martínez, J.; Pulgar, R.; Amalraj, J.; Araya-Maturana, R.; Urra, F.A. A New Quinone-Based Inhibitor of Mitochondrial Complex I in D-Conformation, Producing Invasion Reduction and Sensitization to Venetoclax in Breast Cancer Cells. *Antioxidants* **2023**, *12*, 1597. [[CrossRef](#)]
29. Kumagai, Y.; Shinkai, Y.; Miura, T.; Cho, A.K. The chemical biology of naphthoquinones and its environmental implications. *Annu. Rev. Pharmacol. Toxicol.* **2012**, *52*, 221–247. [[CrossRef](#)]
30. Bolton, J.L.; Trush, M.A.; Penning, T.M.; Dryhurst, G.; Monks, T.J. Role of Quinones in Toxicology. *Chem. Res. Toxicol.* **2000**, *13*, 135–160. [[CrossRef](#)]
31. Patel, O.P.S.; Beteck, R.M.; Legoabe, L.J. Antimalarial application of quinones: A recent update. *Eur. J. Med. Chem.* **2021**, *210*, 113084. [[CrossRef](#)]
32. Zhang, L.; Zhang, G.; Xu, S.; Song, Y. Recent advances of quinones as a privileged structure in drug discovery. *Eur. J. Med. Chem.* **2021**, *223*, 113632. [[CrossRef](#)] [[PubMed](#)]
33. Aouacheria, A.; Néel, B.; Bouaziz, Z.; Dominique, R.; Walchshofer, N.; Paris, J.; Fillion, H.; Gillet, G. Carbazolequinone Induction of Caspase-Dependent Cell Death in Src-Overexpressing Cells. *Biochem. Pharmacol.* **2002**, *64*, 1605–1616. [[CrossRef](#)] [[PubMed](#)]
34. Agarwal, S.K.; Singh, S.S.; Verma, S.; Kumar, S. Antifungal Activity of Anthraquinone Derivatives from *Rheum Emodi*. *J. Ethnopharmacol.* **2000**, *72*, 43–46. [[CrossRef](#)] [[PubMed](#)]
35. Chrysayi-Tokousbalides, M.; Kastanias, M.A. Cynodontin: A Fungal Metabolite with Antifungal Properties. *J. Agric. Food Chem.* **2003**, *51*, 4920–4923. [[CrossRef](#)] [[PubMed](#)]

36. Kim, Y.M.; Lee, C.H.; Kim, H.G.; Lee, H.S. Anthraquinones Isolated from Cassia Tora (Leguminosae) Seed Show an Antifungal Property against Phytopathogenic Fungi. *J. Agric. Food Chem.* **2004**, *52*, 6096–6100. [[CrossRef](#)] [[PubMed](#)]
37. Ferreira, E.S.B.; Hulme, A.N.; McNab, H.; Quye, A. The Natural Constituents of Historical Textile Dyes. *Chem. Soc. Rev.* **2004**, *33*, 329–336. [[CrossRef](#)] [[PubMed](#)]
38. Er, S.; Suh, C.; Marshak, M.P.; Aspuru-Guzik, A. Computational design of molecules for an all-quinone redox flow battery. *Chem. Sci.* **2015**, *6*, 885–893. [[CrossRef](#)]
39. Lee, J.; Kim, H.; Park, M.J. Long-Life, High-Rate Lithium–Organic Batteries Based on Naphthoquinone Derivatives. *Chem. Mater.* **2016**, *28*, 2408–2416. [[CrossRef](#)]
40. Itoigawa, M.; Kashiwada, Y.; Ito, C.; Furukawa, H.; Tachibana, Y.; Bastow, K.F.; Lee, K.-H. Antitumor Agents. 203. Carbazole Alkaloid Murrayquinone A and Related Synthetic Carbazolequinones as Cytotoxic Agents. *J. Nat. Prod.* **2000**, *63*, 3–7. [[CrossRef](#)]
41. Khan, Q.A.; Lu, J.; Hecht, S.M. Calothrixins, a new class of human DNA topoisomerase I poisons. *J. Nat. Prod.* **2009**, *72*, 438–442. [[CrossRef](#)]
42. Bernardo, P.H.; Chai, C.L.L.; Heath, G.A.; Mahon, P.J.; Smith, G.D.; Waring, P.; Wilkes, B.A. Synthesis, electrochemistry, and bioactivity of the cyanobacterial calothrixins and related quinones. *J. Med. Chem.* **2004**, *47*, 4958–4963. [[CrossRef](#)] [[PubMed](#)]
43. Murata, T.; Kohno, S.; Ito, C.; Itoigawa, M.; Sugiura, A.; Hikita, K.; Kaneda, N. Inhibitory effect of carbazolequinone derivatives on lipopolysaccharide and interferon- γ -induced nitric oxide production in mouse macrophage RAW264.7 cells. *J. Pharm. Pharmacol.* **2013**, *65*, 1204–1213. [[CrossRef](#)] [[PubMed](#)]
44. Araya-Maturana, R.; Cassels, B.K.; Delgado-Castro, T.; Hurtado-Guzmán, C.; Jullian, C. Complete assignment of the ^{13}C NMR spectra of a series of 5,8-disubstituted 4,4-dimethylanthracene-1,9,10(4h)-triones. *Magn. Reson. Chem.* **1999**, *37*, 312–316. [[CrossRef](#)]
45. Córdova-Delgado, M.; Fuentes-Retamal, S.; Palominos, C.; López-Torres, C.; Guzmán-Rivera, D.; Ramírez-Rodríguez, O.; Araya-Maturana, R.; Urrea, F.A. Fri-1 is an anti-cancer isoquinolinequinone that inhibits the mitochondrial bioenergetics and blocks metabolic shifts by redox disruption in breast cancer cells. *Antioxidants* **2021**, *10*, 1618. [[CrossRef](#)] [[PubMed](#)]
46. Martínez-Cifuentes, M.; Clavijo-Allancan, G.; Zuñiga-Hormazabal, P.; Aranda, B.; Barriga, A.; Weiss-López, B.; Araya-Maturana, R. Protonation sites, tandem mass spectrometry and computational calculations of o-carbonyl carbazolequinone derivatives. *Int. J. Mol. Sci.* **2016**, *17*, 1071. [[CrossRef](#)]
47. Martínez-Cifuentes, M.; Clavijo-Allancan, G.; Di Vaggio-Conejeros, C.; Weiss-López, B.; Araya-Maturana, R. On-water reactivity and regioselectivity of quinones in C–N coupling with amines: Experimental and theoretical study. *Aust. J. Chem.* **2014**, *67*, 217–224. [[CrossRef](#)]
48. Bodenhausen, G.; Ruben, D.J. Natural abundance nitrogen-15 NMR by enhanced heteronuclear spectroscopy. *Chem. Phys. Lett.* **1980**, *69*, 185–189. [[CrossRef](#)]

Disclaimer/Publisher’s Note: The statements, opinions and data contained in all publications are solely those of the individual author(s) and contributor(s) and not of MDPI and/or the editor(s). MDPI and/or the editor(s) disclaim responsibility for any injury to people or property resulting from any ideas, methods, instructions or products referred to in the content.